Coverage dependence of surface structure and vibration of Cl/Cu(100) compared to Cl/Ni(100)

M. Kiguchi, T. Yokoyama, S. Terada, M. Sakano, Y. Okamoto, and T. Ohta
Department of Chemistry, Graduate School of Science, The University of Tokyo, 7-3-1 Hongo, Bunkyo-ku, Tokyo 113, Japan

Y. Kitajima
Photon Factory, National Laboratory for High Energy Physics, 1-1 Oho, Tsukuba, Ibaraki 305, Japan

H. Kuroda
Research Institute for Science and Technology, Science University of Tokyo, Yamazaki 2641, Noda, Chiba 278, Japan
(Received 3 December 1996; revised manuscript received 2 April 1997)

The coverage dependence of surface structure and vibration was investigated for 0.12- and 0.50-ML Cl adsorbed on Cu(100) by means of temperature-dependent Cl *K*-edge surface-extended x-ray-absorption fine structure. The first-nearest-neighbor Cl-Cu distance was found to be 2.42 ± 0.02 Å for 0.12 ML and 2.39 ± 0.02 Å for 0.50 ML. Moreover, the Cl-Cu chemical bond was revealed to be softer and more anharmonic in the 0.12-ML case than in the 0.50-ML one. The present findings are completely opposite to the previous results on Cl/Ni(100) in which the Cl-Ni bond was found to be elongated, softer, and more anharmonic with the Cl coverage. For the understanding of the different nature of Cl/Cu from Cl/Ni, density-functional calculations were performed for finite surface clusters. The theoretically estimated coverage dependence for the equilibrium distance was very consistent with the experimental results for both Ni and Cu. The different coverage dependences of the bond length and strength between Cl/Ni and Cl/Cu can consequently be ascribed to the different Cl ionicity at the saturation coverage, which originates from the different roles of metal 3*d* bands. [S0163-1829(97)05127-8]

I. INTRODUCTION

Static and dynamical properties of atoms adsorbed on single crystal surfaces often show interesting coverage dependence. Andersson, Karlsson, and Persson[1] studied the coverage dependence of O and S/Ni(100) with the high-resolution electron-energy-loss-spectroscopy method. They found that in the O/Ni(100) system the O-Ni vibrational frequency is significantly reduced with increased O coverage, while in the S/Ni(100) case the S-Ni frequency shift is much smaller than the upper case. Bauschlicher and co-workers[2,3] treated the same systems theoretically using a cluster model. They succeeded in explaining vibrational softening of the O-Ni bond with the O coverage, and also found slight stiffening of the S-Ni bond with S coverage. They ascribed such a different nature between O and S to the different coverage dependence of charge transfer from Ni to adsorbate atoms. In the structural studies based on LEED (low-energy electron diffraction) and SEXAFS (surface-extended x-ray-absorption fine structure) of $p(2\times2)$ and $c(2\times2)$ states; however, neither O nor S adsorbates give any meaningful difference in the adsorbate-substrate bond distance.[4–6]

Very recently, we examined the coverage dependence of the surface structures and vibrational properties of Cl/Ni(100) by means of temperature-dependent Cl *K*-edge SEXAFS, and found that the Cl-Ni vibration is softer and more anharmonic in the 0.50-ML case than in the 0.25-ML one, associated with the elongation of the Cl-Ni bond distance at higher coverage.[7] These findings were explained by the enhancement of the adsorbate-adsorbate repulsive interaction with Cl coverage, as in the case of O/Ni(100). In order to obtain deeper insight into adsorbate-metal substrate bonding, it should be of particular interest to investigate the coverage dependence of Cl/Cu(100) and to compare with the results from Cl/Ni(100), since the surface structures are quite similar to each other.

Thus, in the present study, we have measured and analyzed temperature-dependent Cl *K*-edge SEXAFS spectra of Cl/Cu(100) with 0.12- and 0.50-ML Cl coverages. The surface structure of 0.50-ML Cl/Cu(100) with a $c(2\times2)$ LEED pattern has already been investigated,[8–10] while that of a lower coverage has not been reported yet. The Cl-Cu bond distance, the vibrational amplitude and anharmonicity were obtained for these two samples, and the two-body interatomic potentials were consequently estimated. The present results of Cl/Cu(100) are compared to those of Cl/Ni(100). Density-functional quantum-mechanical calculations were also carried out by employing a metal cluster with different number of adsorbate Cl. Origins of the observed coverage-dependent nature of the Cl-metal bonds in Cl/Ni(100) and Cl/Cu(100) are discussed using the calculated electronic properties.

II. SEXAFS

A. Experiment

A mechanically and electrochemically polished Cu(100) crystal was cleaned in an UHV (ultrahigh vacuum) chamber (the base pressure was less than 1×10^{-8} Pa) by repeated cycles of Ar^+ sputtering and annealing at 900 K.[11,12] A clear (1×1) LEED pattern was observed and both S and Cl contaminations were found to be less than 0.01 ML. The clean Cu(100) crystal was dosed with Cl_2 given by the electrolysis of AgCl in a manner similar to that described previously.[7,13]

Two samples were prepared by Cl_2 dosage at room temperature, and subsequent annealing to 573 K. One corresponds to a saturation coverage (0.50 ML), which gave a clear $c(2\times2)$ LEED pattern. The other gave a lower coverage (0.12-ML Cl), and exhibited only rather a diffuse (1×1) pattern. Here the Cl coverage was estimated from the normalized Cl K fluorescence yield (edge jump), by assuming a Cl coverage of the former sample of 0.50 ML.

Cl K-edge SEXAFS measurements were carried out at the soft-x-ray double-crystal monochromator station BL-11B of the Photon Factory in the National Laboratory for High Energy Physics.[14–16] The factor of linear polarization was estimated to be larger than 0.97 for the monochromatized photons, and the energy resolution of the Ge(111) monochromator was about 1.5 eV around the Cl K-edge region. The fluorescence yield detection method was employed to obtain Cl K-edge SEXAFS data by using an UHV-compatible gas-flow proportional counter with P10 gas (10% CH_4 in Ar) as a detector.[17] The SEXAFS spectra of 0.12- and 0.50-ML Cl/Cu(100) were taken at normal ($\theta=90°$) and grazing ($\theta=15°$) x-ray incident angles. For the normalization of the fluorescence yield, spectra with the intensity of the incident x rays, we measured a drain current from a Cu mesh in the upstream of the sample crystal. The measurements were done at 100 and 300 K. For the measurement at 100 K, the sample crystal was cooled down using a liquid-N_2 cryostat. The sample temperature was monitored with a chromel-alumel thermocouple which was spot welded on a Ta sheet attached to the sample surface. The temperature fluctuations were less than ±3 K during the SEXAFS measurements.

B. Static surface structures

Extraction of the EXAFS function $\chi(k)$ (k is the photoelectron wave number) was carried out according to the well-established procedures: pre- and post-edge background subtractions and subsequent normalization with the atomic absorption coefficients.[18,19] The edge energy E_0 was tentatively chosen as an inflection point of the Cl K edge of the 15° spectrum for each sample. Figures 1 and 2 show the $k\chi(k)$ functions and corresponding Fourier transforms, respectively. The assignments of the Fourier peaks can be performed according to the literature.[6–9] The most noticeable difference between 0.12 and 0.50 ML is found at ~3.3 Å in the Fourier transforms for 90° incidence [compare Fig. 2(c) with Fig. 2(d)]. This peak in Fig. 2(c) is attributed to the Cl-Cl shell. In the 0.50-ML coverage the $c(2\times2)$ overlayer is completed, this leading to an intense Cl-Cl contribution. On the other hand, in the 0.12-ML case [Fig. 2(d)] this peak is not observed, implying that no noticeable formation of the $c(2\times2)$ islands occurs. Another difference between 0.12 and 0.50 ML is observed in the first-nearest-neighbor (NN) Cl-Cu shells appearing at ~2.1 Å. When we compare the low-temperature data at 15° incidence, which give the most intense first-NN contribution [see solid lines of Figs. 2(a) and 2(b)], we find that the 0.50-ML coverage provides a little shorter Cl-Cu distance than the 0.12-ML one, this being quantitatively clarified by the following curve-fitting analysis.

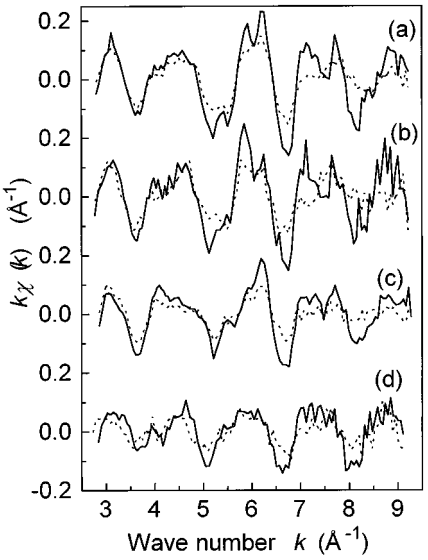

FIG. 1. Cl K-edge EXAFS oscillation functions $k\chi(k)$: (a) 0.50 ML, 15°; (b) 0.12 ML, 15°; (c) 0.50 ML, 90°; (d) 0.12 ML, 90°. The measurement temperatures are 100 K (solid line) and 300 K (dotted line).

The curve-fitting analysis of the first-NN Cl-Cu shells for the 100-K data in the k space was subsequently performed after the Fourier filtering and inverse Fourier transformation, using theoretical standards given by FEFF6.[20] The fitting parameters employed were $N^*S_0^2$ (the effective coordination number N^* multiplied by the intrinsic loss factor S_0^2), R (the interatomic distance), ΔE_0 (the edge energy shift), and C_2 (the mean-square relative displacement). C_2 for the 90° incidence data was consequently fixed to be the same as that for the 15° incidence one to give meaningful values of $N^*S_0^2$.

The results are summarized in Table I, together with the fitting ranges. The first-NN Cl-Cu distance was determined

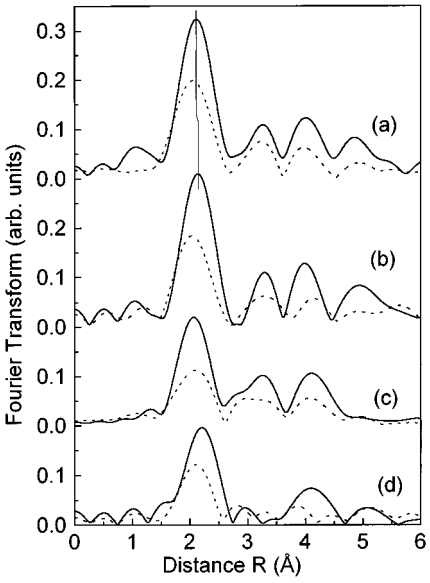

FIG. 2. Fourier transforms of $k\chi(k)$ of Cl/Cu(100): (a) 0.50 ML, 15°; (b) 0.12 ML, 15°; (c) 0.50 ML, 90°; (d) 0.12 ML, 90°. The measurement temperatures are 100 K (solid line) and 300 K (dotted line).

TABLE I. The results of the SEXAFS analysis for the first-NN Cl-Cu shells in the 0.12- and 0.50-ML Cl/Cu(100) states at 100 K. All the fitting k ranges $\Delta k_{\rm fit}$ are 3.2–8.9 Å^{-1}. $N^*S_0^2$, R, ΔE_0, and C_2 are the parameters given by the EXAFS experiments and the FEFF$_6$ standards, while N^* was evaluated from the consequently determined structures.

Coverage (ML)	θ (°)	$\Delta k_{\rm FT}$ (Å^{-1})	ΔR (Å)	NS_0^2	R (Å)	ΔE_0 (eV)	C_2 (10^{-2} Å^2)	N^*
0.12	15	2.85–9.20	1.50–2.80	3.8(5)	2.413(20)	4.3	0.86(9)	5.10
	90	2.85–9.20	1.70–2.80	2.3(4)	2.429(20)	4.3	0.86(9)	2.71
0.50	15	2.80–9.20	1.55–2.70	3.7(5)	2.392(20)	4.3	0.76(8)	5.00
	90	2.80–9.20	1.40–2.70	2.4(4)	2.395(20)	4.3	0.76(8)	3.31

to be 2.42±0.02 Å for 0.12 ML and 2.39±0.02 Å for 0.50 ML, respectively. The Cl-Cu distance of 2.39 Å in the 0.50-ML state is in good agreement with the result of 2.37 ±0.02 Å (at 80 K) given by the previous SEXAFS,[6,8,9] and 2.38±0.05 Å (at 110 K) given by the photoelectron diffraction (PhD) measurements,[21] but is slightly smaller than the value of 2.41±0.02 Å from LEED.[22] Although the distance difference between the 0.12- and 0.50-ML states is within the errors, a higher-coverage state provides a slightly shorter bond distance, as found in the Fourier transforms in Fig. 2. For a better understanding of the distance difference, we show the filtered $k\chi(k)$ functions for the first-NN Cl-Cu shells at 15° x-ray incidence in Fig. 3, which includes temperature dependence discussed below. When the $k\chi(k)$ function at 100 K for the 0.50-ML coverage [the solid curve in Fig. 3(a)] is compared to that for the 0.12-ML one [the solid curve in Fig. 3(b)], the phase for the former is gradually delayed more than that for the latter, implying a shorter Cl-Cu distance in the 0.50-ML coverage.

On the other hand, from the ratios of the effective coordination numbers $N^*(90°)/N^*(15°)$ of 0.62±0.10 for 0.12 ML and 0.66±0.07 for 0.50 ML, adsorption of Cl on the fourfold hollow site can be confirmed in both the states since the expected values of $N^*(90°)/N^*(15°)$ for the hollow site are 0.66 and 0.68, respectively.

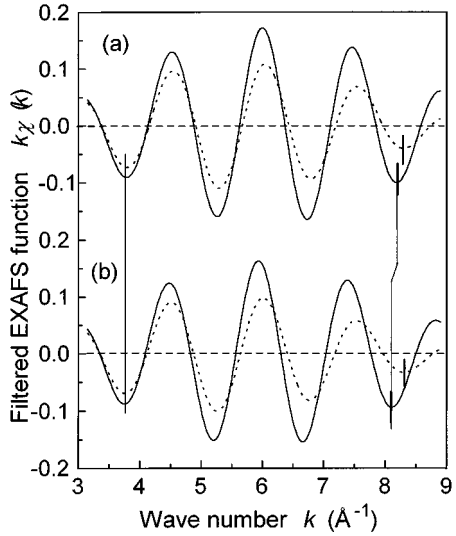

FIG. 3. Filtered $k\chi(k)$ of the first-NN Cl-Cu shells in the 15° incidence data of (a) 0.50 ML and (b) 0.12 ML Cl/Cu(100) taken at the temperatures of 100 K (solid line) and 300 K (dotted line). Some vertical lines are given for easier understanding of the phase delays.

C. Vibrational properties of the surface Cl-Cu bonds

The temperature dependence of the EXAFS spectra for the first-NN Cl-Cu shells was subsequently analyzed. The $\Delta k_{\rm FT}$ and ΔR ranges were the same as the above structural analysis given in Table I. Figure 3 also shows the temperature dependence of the filtered $k\chi(k)$ functions for the first-NN Cl-Cu shells. It is clearly found in both the 0.12- and 0.50-ML states that as the temperature increases the EXAFS amplitude is reduced and the phase is gradually delayed at higher-k regions. The amplitude reduction at higher temperature is the consequence of increase in the mean-square relative displacement C_2 (EXAFS Debye-Waller factor). The phase delay is not caused by the shortening of the Cl-Cu distance at higher temperature but by increase in the mean-cubic relative displacement C_3.[23] One can clearly find that the phase delay at the higher-k region is more enhanced in the 0.12-ML state than in 0.50-ML one, and correspondingly the amplitude reduction is found to be slightly more significant in the 0.12-ML state. This indicates that temperature differences of the cumulants $\Delta C_2(T_1,T_2)$ and $\Delta C_3(T_1,T_2)$ ($T_1=100$ K and $T_2=300$ K) are greater in the 0.12-ML state.

The numerical values of ΔC_2 and ΔC_3 were obtained by the amplitude ratio and phase-difference methods and also the curve-fitting method,[19] where $\Delta k_{\rm fit}$ employed were 3.2–8.9 Å. The results are tabulated in Table II, together with the previous results on Cl/Ni(100) for comparison,[7] which provides more quantitative and detailed information. ΔC_2(100 K, 300 K) for the 0.50-ML state was obtained as 6.2(6) $\times 10^{-3}$ Å^2, which agrees with ΔC_2(80 K, 280 K) of 5.5(5)$\times 10^{-3}$ Å^2 by the previous SEXAFS experiments[6,9] within the errors, and slightly deviates from ΔC_2(110 K, 300 K) of 4.5(4)$\times 10^{-3}$ Å^2 by PhD.[21]

In order to describe the interatomic potentials of the Cl-Cu atom pair, one can simply assume a third-order polynomial within the two-body Einstein approximation as

$$V(r)=\tfrac{1}{2}\alpha(r-r_0)^2-\beta(r-r_0)^3,$$

where α and β are the second- and third-order force constants, respectively, and r_0 the equilibrium distance (potential minimum). The relationship between the EXAFS cumulants and the force constants in the case of the two-body system have been clarified using the first-order quantum-

TABLE II. Results of $\Delta C_2(T_1,T_2)$ and $\Delta C_3(T_1,T_2)$ ($T_1=100$ K, $T_2=300$ K) for the first-NN Cl-Cu shells in 0.12- and 0.50-ML Cl/Cu(100), together with the previous results for the first-NN Cl-Ni bond in Cl/Ni(100) (Ref. 7). The two-body effective potential parameters α, β, and r_0 are also given.

System	Coverage (ML)	ΔC_2 (10^{-3} Å^2)	ΔC_3 (10^{-4} Å^3)	α (mdyn/Å)	β (mdyn/Å^2)	r_0 (Å)
ClCu(100)	0.12	6.8(6)	13.6(27)	0.35(4)	0.65(13)	2.41(2)
	0.50	6.2(6)	7.4(15)	0.38(4)	0.46(10)	2.39(2)
ClNi(100)	0.25	3.7(3)	1.0(2)	0.58(4)	0.21(5)	2.31(2)
	0.50	4.4(3)	2.6(3)	0.51(3)	0.38(6)	2.34(2)

statistical perturbation theory of thermal averages.[24–27] The evaluated results of α and β using ΔC_2 and ΔC_3 are also given in Table II. The second-order force constant α is found to be slightly larger in the 0.50-ML state, while the third-order force constant β is larger in 0.12 ML, implying stiffer vibration and smaller anharmonicity at higher Cl coverage. Although the difference is again not so significant for each value, all the results of R, α, and β consistently indicate that the Cl-Cu bond strength is greater at higher Cl coverage.

Figure 4 shows ΔC_2 and ΔC_3 variations as a function of the Cl-metal (Cu and Ni) distance. It is apparently found that with an elongation of the Cl-metal distance ΔC_2 and ΔC_3 increase monotonically, thus implying that the longer bond is the softer and more anharmonic. The most important finding is the difference of the coverage dependence. As noted in Sec. I, in the previous Cl/Ni(100) system the Cl-Ni bond is noticeably weakened as the Cl coverage increases, while in the present Cl/Cu(100) case the Cl-Cu bond is found to tighten with the Cl coverage. Although each difference in the bond distance, ΔC_2, and ΔC_3 is within the error bars in the case of Cl/Cu(100), all the results suggest a tightening of the Cl-Cu bond with the coverage, which sounds physically significant.

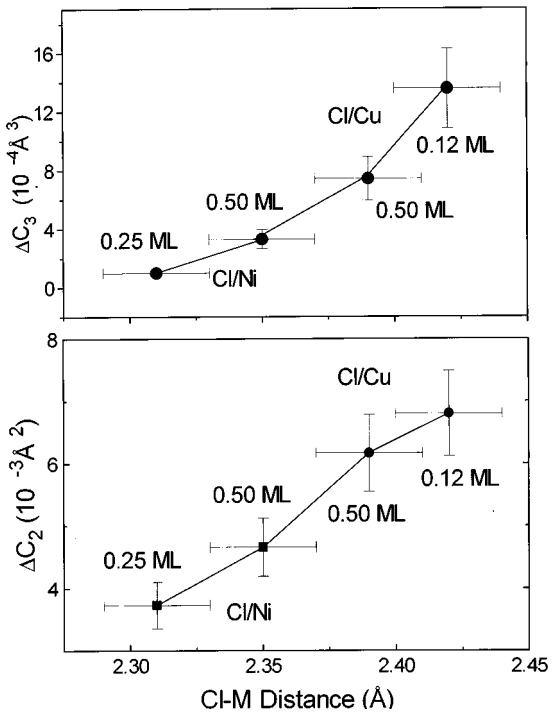

FIG. 4. $\Delta C_2(T_1,T_2)$ and $\Delta C_3(T_1,T_2)$ ($T_1=100$ K and $T_2=300$ K) of Cl/M(100) (M=Ni,Cu) as a function of the Cl-M distance.

III. DENSITY-FUNCTIONAL CALCULATIONS

A. Methods

In order to understand the different coverage dependence between the Cl/Ni(100) and Cl/Cu(100) systems, we performed first-principle quantum-mechanical calculations on the cluster models of those surfaces. The method used was an *ab initio* calculation based on the density-functional theory (DFT). The calculations were done by use of the DFT quantum-mechanical code DMol ver. 950 of Biosym/MSI, by using the double numerical basis functions with polarization function[28–30] as the atomic basis set, and the local-spin-density functional derived by Vosko, Wilk, and Nusair.[31] All inner core levels were frozen in the present calculations.

The cluster model used for the $M(100)$ (M=Ni,Cu) surface was composed of 25 metal atoms, among which 16 M atoms were in the top atomic layer and nine atoms were in the second layer.[2,3,32] The coordination of atoms and all the M-M distances were taken to be the same as in the bulk metal crystal, implying the assumption of unrelaxed and unreconstructed surfaces. In the calculations for the low coverage state (0.12 ML), one Cl atom was placed on the fourfold hollow site at the center of the top atomic layer of the above metal cluster (see Fig. 5). Hereafter we denote this model as the Cl_1M_{25} cluster. Fixing the position of the metal atoms in the ClM_{25} cluster, we calculated the total binding energy as a function of the height of the Cl atom, Z, measured from the top metal atom plane.

For the high-coverage $c(2\times2)$ state, five Cl atoms were put on the five fourfold hollow sites of the top metal atom

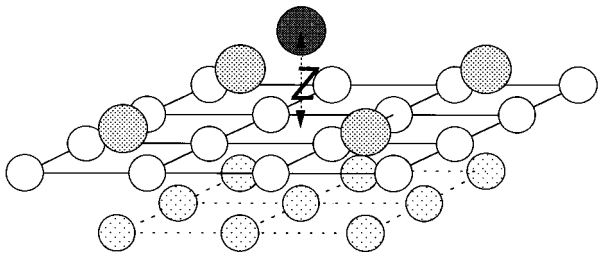

FIG. 5. Schematic view of the Cl_5M_{25} (M=Ni,Cu) cluster. Only the central Cl atom was used for the description of lower coverage, while all the five Cl atoms were included to model the $c(2\times2)$ coverage.

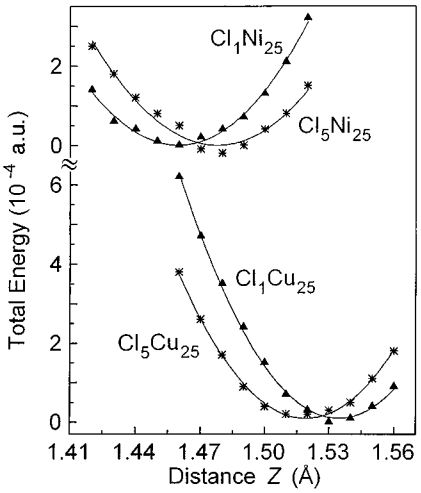

FIG. 6. Potential-energy curves of the Cl_xM_{25} clusters ($x=1,5$; $M=$Ni,Cu) in the vicinity of the equilibrium distance. The minimum of each potential curve was assumed to be the origin of the energy.

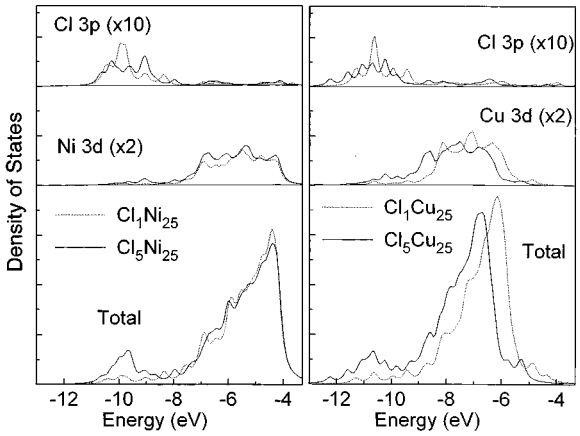

FIG. 7. The total DOS and the partial DOS of metal $3d$ and Cl $3p$ for the Cl_xM_{25} clusters ($x=1$, 5; $M=$Ni,Cu). The partial DOS of Cl $3p$ includes only the one for the central Cl atom, and those of metal $3d$ are derived only from the four first-NN metal atoms which directly interact with the central Cl. The energy is referred to the vacuum level.

plane as shown in Fig. 5. This cluster model is denoted as the Cl_5M_{25} cluster. In this case, the height of the Cl atoms except that of the one at the center were at first taken to be equal to the value found for the most stable state from the calculations on the Cl_1M_{25} cluster. Fixing the positions of metal atoms and four Cl atoms at the surrounding sites, we calculated the total binding energy of the cluster as a function of the height of the central Cl atom. After obtaining the equilibrium distance, the surrounding four Cl atoms were replaced at the optimized positions, and the total-energy calculations were performed once again to verify the equilibrium distance. The distance was found to be completely identical and one does not have to care the slight change of the heights of the surrounding Cl atoms.

B. Results

Let us first discuss the theoretical equilibrium Cl-metal distances. To determine the Cl-metal distances, the total energy curve was calculated as a function of the Cl height Z in the vicinity of the potential minimum, the results being plotted in Fig. 6. Using parabolic fits, the equilibrium distances were finally obtained, and the results are summarized in Table III. The interatomic distance between the central Cl and the first-NN Ni was found to be 2.288 Å for Cl_1Ni_{25} and 2.301 Å for Cl_5Ni_{25}, respectively, while that was 2.371 Å for Cl_1Cu_{25} and 2.358 Å for Cl_5Cu_{25}. These values are close to the experimentally obtained distances of 2.31–2.41 Å, this implying a high reliability of the present density-functional calculations. The sequence of the Cl-metal bond length was well reproduced. The Cl-Ni distance is noticeably shorter (by $\sim$0.07 Å) than the Cl-Cu one, this being consistent with the experimental tendency ($\sim$0.07 Å). For the coverage dependence as well, the calculated results indicate that in the case of Cu the Cl-Cu distance is getting shorter with the Cl coverage, while on Ni the Cl-Ni distance is the longer. This consequence is fully consistent with the experimental findings.

TABLE III. The equilibrium Cl-M ($M=$Cu,Ni) distance $R_{\text{Cl-}M}$ and the Mulliken charge q_{Cl} of Cl, obtained by the density-functional calculations of the Cl_1M_{25} and Cl_5M_{25} clusters.

System	$R_{\text{Cl-}M}$ (Å)	q_{Cl}
Cl_1Cu_{25}	2.371	−0.25
Cl_5Cu_{25}	2.358	−0.13
Cl_1Ni_{25}	2.288	−0.23
Cl_5Ni_{25}	2.301	−0.33

Figure 7 shows the calculated density of states (DOS) of these clusters, where each discrete level has been artificially broadened with the width of 0.2 eV. The energy is the one measured from the vacuum level. In the total DOS, chlorine-derived peaks appear around $\sim$9.7 eV for Cl_5Ni_{25} and $\sim$10.7 eV for Cl_5Cu_{25}, which can be ascribed to the Cl $3p$ components interacting with metal $3d$ bands. Although ultraviolet photoemission spectra (UPS) of Cl/Ni(100) has not been reported to our knowledge, the UPS of Cl/Cu(100) has been studied in detail,[33–36] and shows a Cl $3p$ peak at $\sim$5 eV below the Fermi level E_F. Since the present calculations gave a work function of 5.2 eV for Cl_5Cu_{25}, the theoretical energy level of Cl $3p$ (5.5 eV in regard to E_F) is found to provide good agreement with the experiment. The overall features of the calculated spectrum of Cl_5Cu_{25} are also consistent with the experiment, this indicating that our cluster model has picked up the surface state properly.

Figure 7 also shows the partial DOS of Cl $3p$ (only for central Cl) and metal $3d$ bands. A clear difference in the coverage dependence between Cl_xNi_{25} and Cl_xCu_{25} can be detected. On the Cu substrate, the components of both Cl $3p$ and Cu $3d$ as well as the total DOS are found to shift to a higher-binding-energy side as the Cl coverage increases. On the other hand, on the Ni substrate, no significant coverage dependence can be found in the partial DOS of Ni $3d$ or the total DOS. In the Cl $3p$ levels, a single dominant contribution is seen at $\sim$10 eV for Cl_1Ni_{25}, while for Cl_5Ni_{25} this contribution is spread into several peaks. It should be noted

that one of the Cl $3p$ levels for Cl_5Ni_{25} is located at a low-binding-energy side of ~ 9.1 eV, yielding the lower-energy shift of the whole Cl $3p$ levels. This indicates that the increase in the Cl coverage induces the weakening of the Cl-Ni bonds.

Table III gives the Mulliken charges of the central Cl atom. One can find that by comparing the results of Cl_1Ni_{25} and Cl_1Cu_{25}, the ionicity of Cl does not change at a low Cl coverage between Ni and Cu. This is reasonable, since the electronegativities of Ni and Cu are almost equal to each other. The coverage dependence is, however, significantly different. The Cl ionicity is enhanced on Ni with the coverage, while on Cu the ionicity is reduced. As mentioned in Sec. I, similar findings have been reported by Bauschlicher and co-workers[2,3] on the O/Ni and S/Ni systems. According to their molecular-orbital calculations of model clusters, charges on O and S on Ni(100) are almost the same at low coverage. On increasing the coverage, however, O becomes more negatively charged, while S becomes less ionic though the effect on S is small. The trend resembles the present findings.

IV. DISCUSSION

As a consequence of the previous experimental and theoretical sections, the observed coverage dependence of the interatomic distance $R_{\text{Cl-}M}$, the second-order force constant α, and the third-order constant (anharmonicity) β in the Cl/Ni(100) and Cl/Cu(100) systems could be ascribed to the variation of the Cl charge q_{Cl} obtained theoretically. Let us consider two different chemical interactions of ionic and covalent bonds. The decrease in ionicity implies the enhancement of the covalent nature, as long as the chemical bond is preserved. In general, since the ionic and covalent attractive interactions are long- and short-range forces, respectively, the curvature of the ionic potential should be looser than that of the covalent one. This leads to smaller α and β in more ionic interaction, being consistent with the present experimental findings. For the Cl-metal distances as well, it can be remarked that the more covalent the interaction, the shorter the bond length, because the covalent interaction requires more significant overlap between the atomic orbitals than the ionic one (in other words, covalent radii are smaller than ionic radii). This is also consistent with the experimental and theoretical results.

A remaining question might be why the Cl charge exhibits such a drastic difference in the coverage dependence between Ni and Cu. This should originate from the different chemical interactions between the Cl-Ni and Cl-Cu bonds. Since Ni is a transition-metal element, N; $3d$ orbitals dominantly participate in the Cl-Ni bond formation. On the other hand, Cu $3d$ orbitals located at higher binding energies are fully occupied and are less important for the Cl-Cu bond. Instead, the Cu $4s$ level interacts with Cl $3p$. Since the $3d$ orbital is much more localized than the $4s$ orbital, the chemical bond for the Cl-Ni pair is stronger than that for the Cl-Cu pair. This was clearly demonstrated by the present SEXAFS results (see Table II).

For discussing the coverage dependence, it might be complicated to consider the interaction between the neutral Cl and the metal surface, since Cl plays significant roles of both electron donor and acceptor. Thus let us here consider the interaction between Cl^- anion and the cationic metal surface. As the Cl coverage increases, the electron of Cl^- is donated to the Cu $4s$ band in the Cl/Cu system, while that is donated mainly to the Ni $3d$ band in Cl/Ni. Since the Cu $4s$ band is broadened and is of less density in the vicinity of the Fermi level, the increase in electrons should shift the Fermi level (work function) of the Cu metal significantly. On the other hand, because of a high density of the Ni $3d$ band, the Fermi level does not change so much for the Ni metal. These remarks are actually found in Fig. 7.

There should be two competing repulsive forces in the case of high-coverage Cl adsorption. One is the Cl-Cl repulsive Coulomb force, and the other is the electron-electron repulsion in the metal bands. In the case of Cu, the electrons from Cl^- are transferred into the Cu $4s$ band, and the electron-electron repulsion is less important because of the free-electron-like nature of the $4s$ band, implying that the Cl-Cl Coulomb interaction should be a dominant repulsive force. Consequently, so as to reduce the Cl-Cl repulsion, the charge transfer from Cl^- to the Cu $4s$ band is more enhanced with the increase in the Cl coverage. On the other hand, in the case of Ni, the electrons from Cl^- should be localized in the Ni $3d$ band, and the electron-electron repulsion might play a more significant role upon the charge transfer from Cl^- to Ni metal. Accordingly, in spite of the increase in the Cl^- coverage, the Ni $3d$ band could not accept the electrons from Cl^- to any great degree. The charge of the Cl anions resultantly remains more with the coverage increase, as given in Table III. The difference of the coverage dependence of Cl between Ni and Cu metal surfaces has thus been recognized.

V. CONCLUSIONS

We have measured and analyzed temperature dependence of Cl K-edge SEXAFS spectra of the 0.12- and 0.50-ML Cl/Cu(100) states. Local surface structures have been found to be almost identical with each other, except for the presence of the Cl-Cl coordination in the 0.50-ML $c(2\times 2)$ state. The first-NN Cl-Cu bond distance is, however, slightly different: 2.42 ± 0.02 Å for 0.12 ML and 2.39 ± 0.02 Å for 0.50 ML. The harmonic force constant is smaller and the anharmonicity is greater in the 0.12-ML state than in the 0.50-ML state. These experimental results clearly demonstrate that the Cl-Cu bond is tightened with the Cl coverage, such a coverage dependence being opposite to that in the Cl/Ni(100) system. Density-functional calculations have been carried out using finite cluster models of Cl_xNi_{25} and Cl_xCu_{25} ($x=1$ and 5). The tendency of the coverage dependence was reproduced well from the view point of the Cl-metal equilibrium distance. Different coverage dependence was also clearly found in the DOS.

The observed coverage dependence of the distance, vibrational amplitude, and anharmonicity for the Cl-metal bonds in Cl/Ni(100) and Cl/Cu(100) was consequently ascribed to the variation of the ionicity of the Cl atom. As the Cl coverage increases, the Cl ionicity is enhanced in the case of Ni,

while it is reduced in the Cu case. The latter implies an enhancement of the covalency for the Cl-Cu bond, leading to a shorter bond distance and a larger force constant with the Cl coverage. The drastic difference between Ni and Cu was also explained by the different nature of the chemical interactions between Cl-Ni and Cl-Cu pairs; upon the formation of the Cl-metal bonds, the Cl $3p-$Ni $3d$ interaction plays a dominant role for the Cl-Ni bond, while for the Cl-Cu one the Cl $3p-$Cu $4s$ is important. This yields a different ionicity of Cl between Ni and Cu at saturation coverage. The present Cl/Ni and Cl/Cu systems have provided excellent examples for the coverage dependence of the adsorbate-substrate bond.

ACKNOWLEDGMENTS

The authors are grateful for the financial support of a Grant-in-Aid for Scientific Research from the Ministry of Education in Japan (No. 07454060). A part of this work was performed under the approval of Photon Factory Program Advisory Committee (PF-PAC No. 95-G379).

[1] S. Andersson, P.-A. Karlsson, and M. Persson, Phys. Rev. Lett. **51**, 2378 (1983).
[2] P. S. Bagus, H. F. Schaefer, and C. W. Bauschlicher, Jr., J. Chem. Phys. **78**, 1390 (1983).
[3] C. W. Bauschlicher and P. S. Bagus, Phys. Rev. Lett. **54**, 349 (1985).
[4] J. Stöhr, R. Jaeger, and T. K. Kendelewicz, Phys. Rev. Lett. **49**, 142 (1982).
[5] M. Van Hove and S. Y. Tong, J. Vac. Sci. Technol. **12**, 230 (1975).
[6] F. Sette, T. Hashizume, F. Comin, A. A. MacDowell, and P. H. Citrin, Phys. Rev. Lett. **61**, 1384 (1988).
[7] T. Yokoyama, S. Terada, Y. Okamoto, M. Sakano, T. Ohta, Y. Kitajima, M. Tischer, and K. Baberschke, Surf. Sci. **374**, 243 (1997).
[8] P. H. Citrin, D. R. Hamann, L. H. Mattheis, and J. E. Rowe, Phys. Rev. Lett. **49**, 1712 (1982).
[9] F. Sette, C. T. Chen, J. E. Rowe, and P. H. Citrin, Phys. Rev. Lett. **20**, 311 (1987).
[10] J. R. Patel, D. W. Berreman, F. Sette, P. H. Citrin, J. E. Rowe, P. L. Cowan, T. Jach, and B. Karlin, Phys. Rev. B **40**, 1330 (1989).
[11] S. Yagi, T. Yokoyama, Y. Kitajima, Y. Takata, T. Kanazawa, A. Imanishi, and T. Ohta, Surf. Sci. **311**, 172 (1994).
[12] S. Yagi, S. Takenaka, T. Yokoyama, Y. Kitajima, A. Imanishi, and T. Ohta, Surf. Sci. **325**, 68 (1995).
[13] N. D. Spencer, P. J. Goddard, P. W. Davies, M. Kiston, and R. M. Lambert, J. Vac. Sci. Technol. A **1**, 1554 (1983).
[14] T. Ohta, P. M. Stefan, M. Nomura, and H. Sekiyama, Nucl. Instrum. Methods Phys. Res. A **246**, 373 (1986).
[15] M. Funabashi, M. Nomura, Y. Kitajima, T. Yokoyama, T. Ohta, and H. Kuroda, Rev. Sci. Instrum. **60**, 1983 (1989).
[16] Y. Kitajima, J. Electron Spectrosc. Relat. Phenom. **80**, 405 (1996).
[17] M. Funabashi, T. Ohta, T. Yokoyama, Y. Kitajima, and H. Kuroda, Rev. Sci. Instrum. **60**, 2505 (1989).
[18] See, for instance, *X-ray Absorption: Principles, Applications, Techniques of EXAFS, SEXAFS and XANES*, edited by D. C. Koningsberger and R. Prins (Wiley, New York, 1988).
[19] T. Yokoyama, H. Hamamatsu, and T. Ohta, EXAFSH version 2.1, The University of Tokyo, 1993.
[20] S. I. Zabinsky, J. J. Rehr, A. Ankdinov, R. C. Albers, and M. J. Eller, Phys. Rev. B **52**, 2995 (1995).
[21] D. Arvanitis and K. Baberschke, J. Electron Spectrosc. Relat. Phenom. **75**, 149 (1995).
[22] F. Jona, D. Westphal, A. Goldmann, and P. M. Marcus, J. Phys. C **16**, 3001 (1983).
[23] G. Bunker, Nucl. Instrum. Methods Phys. Res. **207**, 437 (1983).
[24] H. Rabus, Ph.D. thesis, Department of Physics, Freie Universität Berlin, 1991 (unpublished).
[25] A. I. Frenkel and J. J. Rehr, Phys. Rev. B **48**, 585 (1993).
[26] T. Yokoyama, K. Kobayashi, T. Ohta, and A. Ugawa, Phys. Rev. B **53**, 6111 (1996).
[27] T. Yokoyama, H. Hamamatsu, Y. Kitajima, Y. Takata, S. Yagi, and T. Ohta, Surf. Sci. **313**, 197 (1994).
[28] B. Delley, J. Chem. Phys. **92**, 508 (1990).
[29] B. Delley, J. Chem. Phys. **94**, 7245 (1991).
[30] B. Delley, D. E. Ellis, A. J. Freeman, E. J. Baerends, and D. Post, Phys. Rev. B **27**, 2132 (1983).
[31] S. J. Vosko, L. Wilk, and M. Nausair, Can. J. Phys. **58**, 1200 (1980).
[32] B. C. Laskowski and P. S. Bagus, Surf. Sci. **138**, L142 (1984).
[33] D. Westphal and A. Goldmann, Surf. Sci. **131**, 91 (1983).
[34] D. Westphal and A. Goldmann, Surf. Sci. **131**, 113 (1983).
[35] D. Westphal and A. Goldmann, Surf. Sci. **133**, 38 (1983).
[36] D. Westphal and A. Goldmann, Solid State Commun. **35**, 437 (1981).